

# Additive manufacturing of electrochemical interfaces : simultaneous detection of biomarkers

Ho, Eugene Hong Zhuang; Ambrosi, Adriano; Pumera, Martin

2018

Ho, E. H. Z., Ambrosi, A., & Pumera, M. (2018). Additive manufacturing of electrochemical interfaces: Simultaneous detection of biomarkers. *Applied Materials Today*, 12, 43-50.  
doi:10.1016/j.apmt.2018.03.008

<https://hdl.handle.net/10356/85919>

<https://doi.org/10.1016/j.apmt.2018.03.008>

---

© 2018 Elsevier Ltd. All rights reserved. This paper was published in *Applied Materials Today* and is made available with permission of Elsevier Ltd.

*Downloaded on 20 Mar 2024 20:28:48 SGT*

# Additive Manufacturing of Electrochemical Interfaces: Simultaneous Detection of Biomarkers

*Eugene Ho Hong Zhuang, Adriano Ambrosi and Martin Pumera\**

Division of Chemistry & Biological Chemistry, School of Physical Mathematical Science,  
Nanyang Technological University, Singapore 637371, Singapore

\*Email: [pumera.research@gmail.com](mailto:pumera.research@gmail.com)

## ABSTRACT

3D-printed stainless steel helical shaped electrodes with or without surface modification with a gold (Au) film, are tested as novel electrode materials for the electrochemical detection of AA and UA in aqueous solutions. Their performance in terms of sensitivity, selectivity and reproducibility is evaluated and compared to conventional glassy carbon electrode (GCE). Owing to the excellent electrocatalytic properties of the 3D-printed gold (Au) electrode, a clear separation between the anodic oxidation signal of ascorbic acid and uric acid in differential pulse voltammogram (DPV) could be obtained, allowing simultaneous quantification of these biomarkers. The oxidation current obtained using the 3D-printed Au electrode increased linearly with its respective biomarkers concentration in the range of 0.1 mM to 1 mM. Furthermore, the 3D-printed Au electrode generally performed better in term of sensitivity and detection limits as compared to GCE. A real sample analysis of Vitamin C tablet (500 mg), *Vitacimin* were conducted using the 3D-printed Au electrode obtaining a variation from claimed concentration of ascorbic acid of only about 0.5%. Therefore,

electrodes fabricated by 3D printing would certainly represent a viable alternative to conventional electrodes for efficient electrochemical analysis in the future.

**KEYWORDS:** 3D-printing, electrochemistry, electroplating, gold electrode, ascorbic acid, uric acid.

Ascorbic Acid (AA), also commonly known as, Vitamin C, is a water soluble organic compound that is highly essential and vital to the human biological system [1]. Ascorbic acid is found in the human body, generally in leukocytes, liver, anterior pituitary lobe as well as in the mammalian brain along with numerous neurotransmitter amines [2]. This organic compound mainly acts as an antioxidant which is highly responsible for several biological metabolisms and hormone synthesis [3,4]. Hence AA supplements are often consumed to prevent gingivitis, scurvy and many other vitamin C deficiency complications [4]. Uric Acid (UA) is generated as an end-product of purine metabolism in the human biological system [5]. The normal concentration of UA in blood serum is approximately in the range of 0.24 – 0.52 mM [6]. Various diseases such as gout, hyperuricemia and arthritis develop when UA exceed its abnormal level. Therefore, effective, and rapid detection of UA and AA is needed and is of great importance in medical diagnosis. Many different analytical methods, such as, high performance liquid chromatography (HPLC)[7], Chemiluminescence [8] and chemometric spectrophotometry [9] have been employed in quantifying and differentiating UA and AA apart. However, in the recent years, electrochemical methods have increased in demand as they exhibit several advantages over those conventional methods such as a simpler instrumentation set up, higher sensitivity, is less costly and available for in-situ measurement [10-12].

The only major drawback in electrochemical methods is that, the oxidation potential of AA and UA on conventional carbon based electrodes, such as glassy carbon electrode (GCE), is relatively close, posing a great challenge for their simultaneous determination [13-15]. Hence, various electrode modifications such as improvising enzymatic material on GCE[16], using nafion film modified ion-exchange membranes electrode[17], and doping nano-particles on graphene oxide/GCE (GO/GCE)[18-21] have been proposed to obtain the separation of the oxidative signals of these biomarkers in a voltammetric measurement. In particular, gold (Au) nanoparticles were found to exhibit excellent electrocatalytic kinetics owing to the unique nanostructure arrangement, high conductivity properties and excellent biocompatibility [22-25].

However, there are still various obvious limitations in the electrode modification. The fabrication, preparation and drop casting process of the electrode would sometimes prove to be very complex, tedious, and time-consuming [26-28].

3D-printing, being one of the more prominent advancing technologies [29], could enable the fabrication of customizable electrode of different design and materials so that efficient analytical devices can be developed. The combination of metal 3D-printing with also surface modification by electroplating has already demonstrated potentiality for example for the detection of DNA hybridization [30], contaminants [31-33], bioactive molecules [34], as well as for energy related applications [35, 36].

We, therefore, explore here the possibility of using stainless steel electrodes fabricated through metal 3D-printing and surface modified with an Au film by means of electrodeposition, for the detection and quantification of the two most commonly known biomarkers, AA, and UA.

## RESULTS AND DISCUSSIONS

Figure 1 summarizes the electrode fabrication process which starts with the electrode design obtained by means of CAD software. Following this design the metal 3D printer produces a series of electrodes in stainless steel. The steel electrodes can successively be modified by electroplating. Here gold plating procedure was employed to cover the electrode surface with a thin Au film. The as printed steel electrode and the gold plated electrodes were coupled with copper wire to ensure electrical connection with the electrochemical analyser and then tested against GCE conventional electrode for the analysis of AA and UA. The physical appearance of the 3D-printed steel electrode changes from a shiny silver shade to a golden hue upon the electrodeposition of Au. Electrode chemical composition was confirmed by scanning electron microscopy (SEM) coupled with energy dispersive X-ray spectroscopy (EDX) as illustrated in Figure 2.

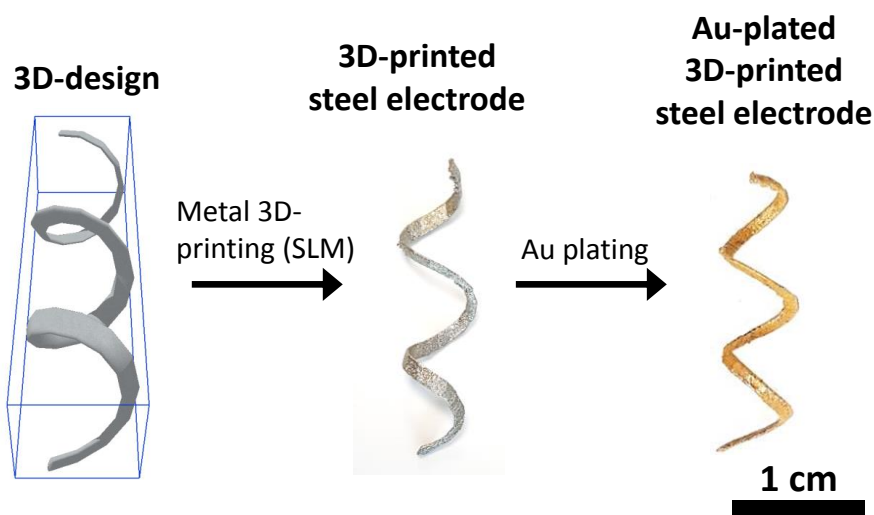


**Figure 1.** Schematic of the metal 3D-printed electrode fabrication and modification.

SEM image of the 3D-printed steel presents a rather rough surface. EDX were used to examine the element composition of the fabricated 3D-printed electrode. It can be seen that

the 3D-printed steel electrode is made mainly of iron (Fe) and nickel (Ni) as expected main steel components (Figure 2A). Subsequently, Au electrodeposition on the 3D-printed steel electrode was conducted and from the SEM images, we could clearly observe that a layer of Au film covers the surface of the electrode causing the physical appearance to change drastically. EDX analysis confirmed the homogeneous distribution of the Au film on the electrode surfaces. Fe and Ni were also detected although with less intense signals due to the covering Au layer (Figure 2B) . With the homogeneous distribution of the Au film it should be expected that the electrode performs similarly to conventional Au electrodes.

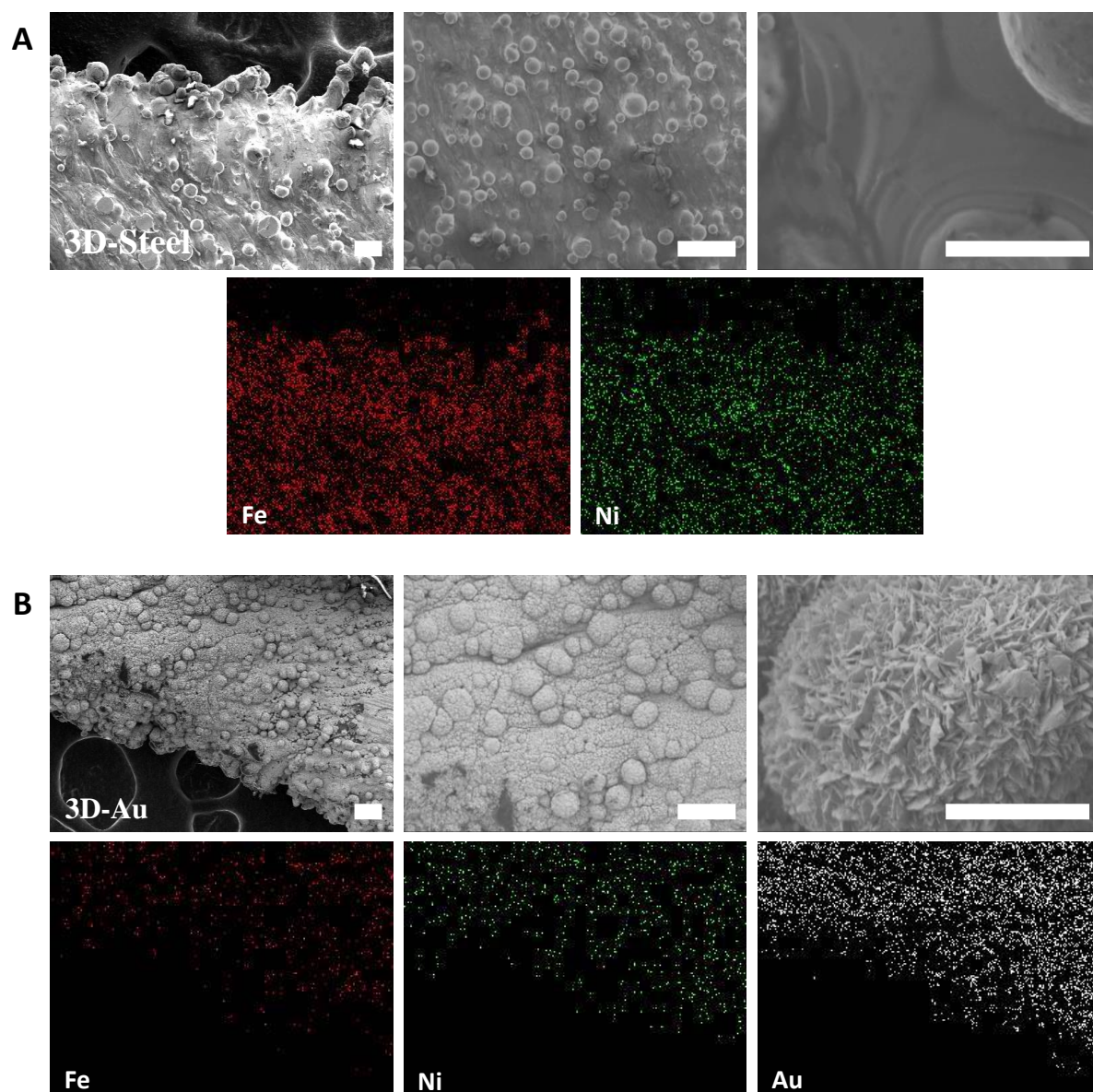


**Figure 2.** SEM images (top) and EDX element mapping (bottom) of a segment of A) 3D-printed steel electrode as-printed and B) after Au electrodeposition. Scale bars from left to right correspond to 100  $\mu\text{m}$ , 100  $\mu\text{m}$  and 10  $\mu\text{m}$ , respectively.

The detection and quantification of biomarkers was first investigated using cyclic voltammetry (CV). Figure 3 shows the cyclic voltammograms recorded with the three electrodes (3D-steel, 3D-Au and GCE) in the presence of ascorbic or uric acid in phosphate buffered solution. It can be seen in Figure 3A that 3D-steel electrode showed inherent redox behaviour with the appearance of oxidation and reduction signals at about -0.45 V, -0.25 V, 0.07 V and 0.73 V even in the absence of the analyte. These are due to the oxidation of Fe and Ni to their ionic states. No additional oxidation signal appeared using this electrode with the addition of AA or UA suggesting that this material is not appropriate for the detection of these biomarkers. The redox behaviour of AA and UA using the gold plated 3D-printed electrode and the glassy carbon electrode (GCE) was investigated by CV in 0.1 M PBS (pH 7.2). In the case of AA, as shown in Figure 3B and 3C, the single anodic oxidation peak that was observed corresponds to the hydroxyl groups that were being oxidised to carbonyl groups in the furan rings. The oxidation reaction of AA is known to be irreversible as the oxidised product, DHAA does not get reduced back, therefore no reduction peak was observed in the CV voltammogram [37]. The anodic oxidation signal of AA at about 350 mV (vs Ag/AgCl) observed using GCE shifted to the value of 20 mV when 3D-printed Au electrode was used. Such significant oxidation potential shift ( $\Delta E_{pa} = 336$  mV) is attributed to the catalytic properties of the Au film. Similarly, for UA, only a single anodic oxidation peak was observed using 3D-printed Au and GCE electrode. UA is known to undergo EC mechanism pathway by which is firstly oxidised to an unstable species, quinonoid, on the electrode surface, followed by a rapid conversion to a tertiary alcohol or carboxylic acid by reacting with surrounding water molecules. Hence, very often the reduction cathodic peak of UA is relatively small or not observable as compared to the oxidation anodic peak [38,39]. Although less significant than for the case of AA, an anodic oxidation potential shift was also experienced with UA when using 3D-printed Au electrode. The oxidation potential of 420

mV recorded with GCE shifted to the lower value of 350 mV using 3D-printed Au electrode which demonstrated therefore catalytic properties for the oxidation of UA. It should be noticed that GCE has shown a relatively small potential separation between AA and UA ( $\Delta E_{UA-AA} = 67$  mV), which indicates that GCE could not be appropriate for simultaneous detection of both analytes. On the other hand, 3D-printed Au electrode displayed a wide potential difference ( $\Delta E_{UA-AA} = 335$  mV), for the detection of AA and UA which can enable their simultaneous determination.

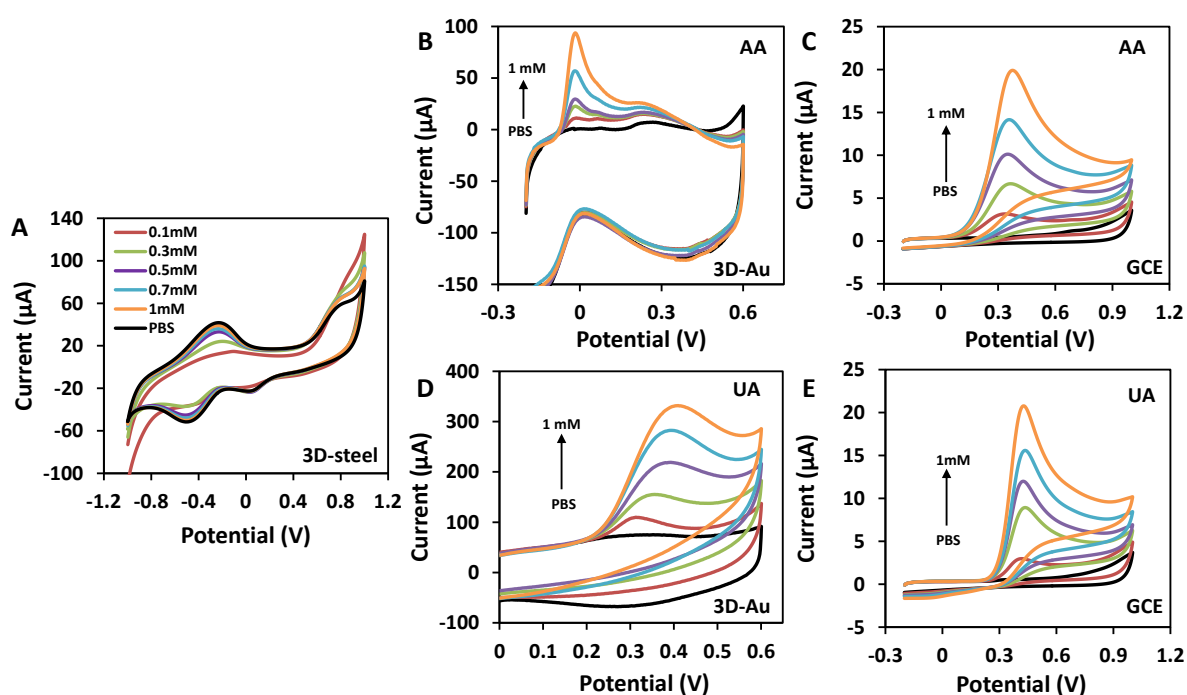


**Figure 3.** A) Cyclic voltammograms recorded with 3D-printed steel electrode with addition of different AA (or UA) concentration (0.1 mM, 0.3 mM, 0.5 mM, 0.7 mM and 1 mM) in 0.1 M PBS (pH 7.2). Cyclic voltammograms recorded at different AA concentrations using B) 3D-printed Au electrode and C) GCE. CV profile of different concentration of UA (0.1 mM, 0.3 mM, 0.5 mM, 0.7 mM and 1 mM) in 0.1 M PBS (pH 7.2) on D) 3D-printed Au electrode E) GCE.

Differential pulse voltammetry (DPV) was employed to investigate the various analytical parameters such as the sensitivity and selectivity of the electrode on individual biomarkers. The DPV voltammograms for AA obtained with GCE and 3D-printed Au electrode is presented in Figure 4. It is clearly observed that the oxidation potential of AA on 3D-printed Au electrode ( $E_p = -60$  mV) is significantly lower than on GCE ( $E_p = 250$  mV), which once again, justify that the 3D-printed Au electrode exhibit better electrocatalytic properties than GCE. For a better comparison electrochemical active surface area was measured for the 3D-printed Au electrode as shown in Supporting Information (Figure S1) obtaining the value of  $55 \text{ mm}^2$ . Geometrical surface area was instead considered for GCE. Taking into account the respective electrode surface area, calibration curves were plotted (Figure 4C and 4D). It can be seen that the 3D-printed Au electrode performs better than the GCE in terms of sensitivity. Other parameters are summarized in table 1. The LOD for AA was determined by employing the respective slope of calibration curve with the existing standard deviation of the lowest available AA concentration (0.1 mM). It was found that the 3D-printed Au electrode can detect lower AA concentration than as compared to GCE. However, relative standard deviation (%RSD) of GCE was found to be marginally lower than the 3D-printed Au electrode by about 5% which indicate that GCE was providing a more consistent and higher repeatability in the electrochemical measurement as compared to the 3D-printed Au electrode. In terms of the linearity of the response, the 3D-printed Au electrode and GCE were almost indistinguishable. Therefore, in the aspect of asynchronous detection of AA, the 3D-printed Au electrode was found to be more effective and sensitive as compared to GCE.

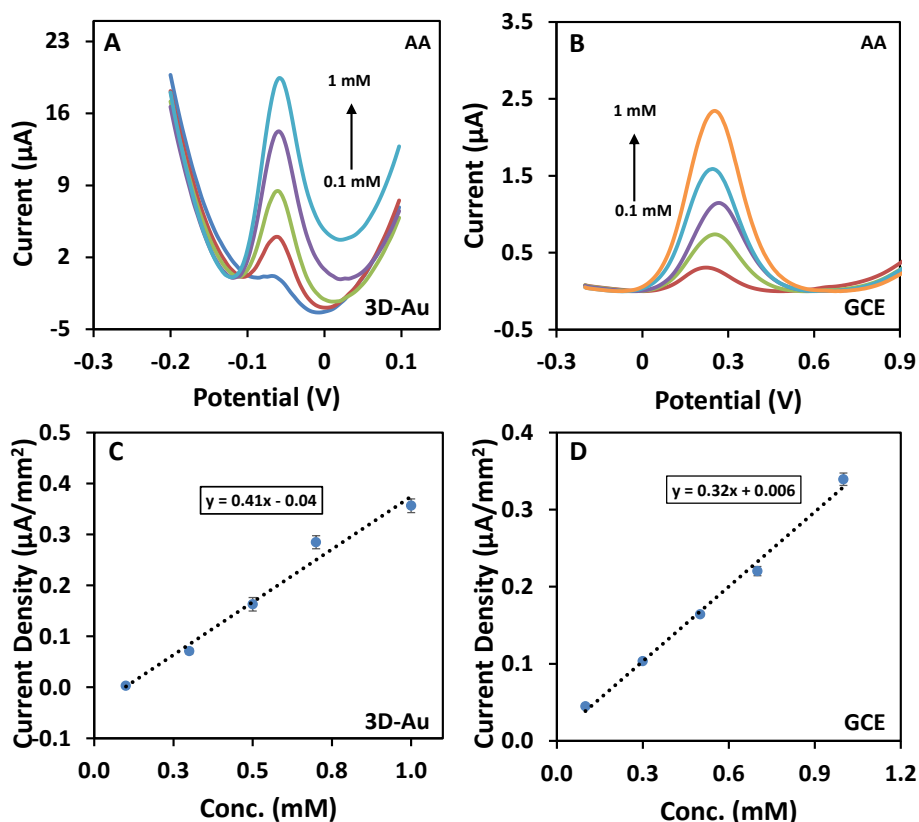


**Figure 4.** DPV profile at different concentration of AA (0.1 mM, 0.3 mM, 0.5 mM, 0.7 mM and 1 mM) in 0.1 M PBS (pH 7.2) on A) 3D-printed Au electrode and B) GCE. Plots of the current density signal as a function of AA concentration (0.1 mM to 1mM) with error bars for C) 3D-printed Au electrode and D) GCE.

DPV measurements were carried out also for UA (Figure 5). The oxidation potential of UA on 3D-printed Au electrode ( $E_p = 308 \text{ mV}$ ) was found to be slightly lower ( $\Delta E_p = 33 \text{ mV}$ ) than GCE ( $E_p = 341$ ). Hence the electron transfer with regards to oxidation of UA on the Au film surface is slightly more efficient as compared to GCE. This result confirms the feasibility of using the 3D-printed Au electrode for the simultaneous determination of AA and UA in the same sample. On the contrary, due to the vicinity of the oxidation potentials recorded with GCE for UA and AA, this electrode cannot be applied for simultaneous

detection. It was observed that oxidation peak current density of UA is proportional to the concentration of UA (0.1 mM to 1 mM) with relatively similar regression coefficient. The slope obtained from 3D-printed Au electrode of UA is approximately 1.1 times higher than of GCE, as shown in Figure 5C and 5D and Table 1. Hence, simply based on the magnitude of the slope, 3D-printed Au electrode exhibited slightly higher responsiveness in detecting UA as compared to GCE. Moreover, in the aspect of %RSD, the 3D-printed Au electrode exhibited a better repeatability and precision than of GCE. However, the LOD of UA on 3D-printed Au electrode was found to be moderately poorer than of GCE.

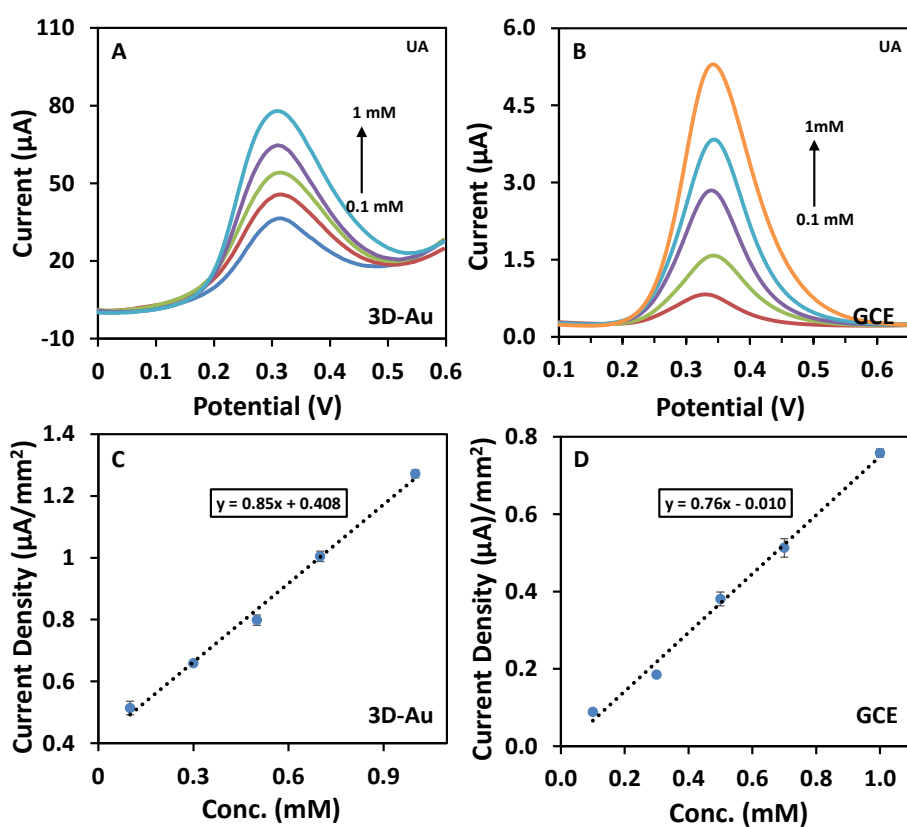


**Figure 5.** DPV profile at different concentration of UA (0.1 mM, 0.3 mM, 0.5 mM, 0.7 mM and 1 mM) in 0.1 M PBS (pH 7.2) on A) 3D-printed Au electrode and B) GCE. Plots of the current density signal as a function of UA concentration (0.1 mM to 1mM) with error bars for C) 3D-printed Au electrode and D) GCE.

**Table 1. Sensitivity, correlation regression coefficient, and limit of detection of DPV of uric acid, with respective working electrodes based on calibration graph plotted.**

Electrode	Analyte	Slope ( $\mu\text{A}/\text{mM mm}^2$ )	LOD ( $\mu\text{M}$ )	RSD (%)	R
GCE	AA	0.32	2.2	2.0	0.997
	UA	0.76	20.4	3.8	0.996
3D-printed Au	AA	0.41	2.1	7.0	0.989
Electrode	UA	0.85	84.0	2.0	0.997

### ***Simultaneous determination of Ascorbic Acid and Uric Acid***

Simultaneous detection of AA and UA was conducted by increasing solely one biomarker concentration while maintaining the other biomarker concentration fixed during every voltammetry scan. As such, any matrices effect that might be affecting the measurement would be evaluated. Based on the voltammogram in Figure 6A, only a broad single peak was observed on GCE as the oxidation potential window of AA and UA were relatively close. GCE therefore cannot be used to distinguish between AA and UA. Such phenomenon was not observed on the 3D-printed Au electrode. Figure 6B shows the DPV curve recorded with increasing AA concentration in the presence of constant UA concentration (0.1 mM). The voltammogram demonstrated that the increment oxidation peaks of AA at its less positive potential window ( $E_p = -47 \text{ mV}$ ) were well separated ( $\Delta E_{\text{UA-AA}} = 355 \text{ mV}$ ) from the peaks of UA ( $E_p = 308 \text{ mV}$ ). Similarly, the DPV curve of increasing UA concentration in the presence

of fixed AA concentration (0.1 mM) presents the oxidation potential peaks of AA ( $E_p = 1$  mV) and UA ( $E_p = 316$  mV) well separated ( $\Delta E_{UA-AA} = 315$  mV) upon the utilising 3D-printed Au electrode.

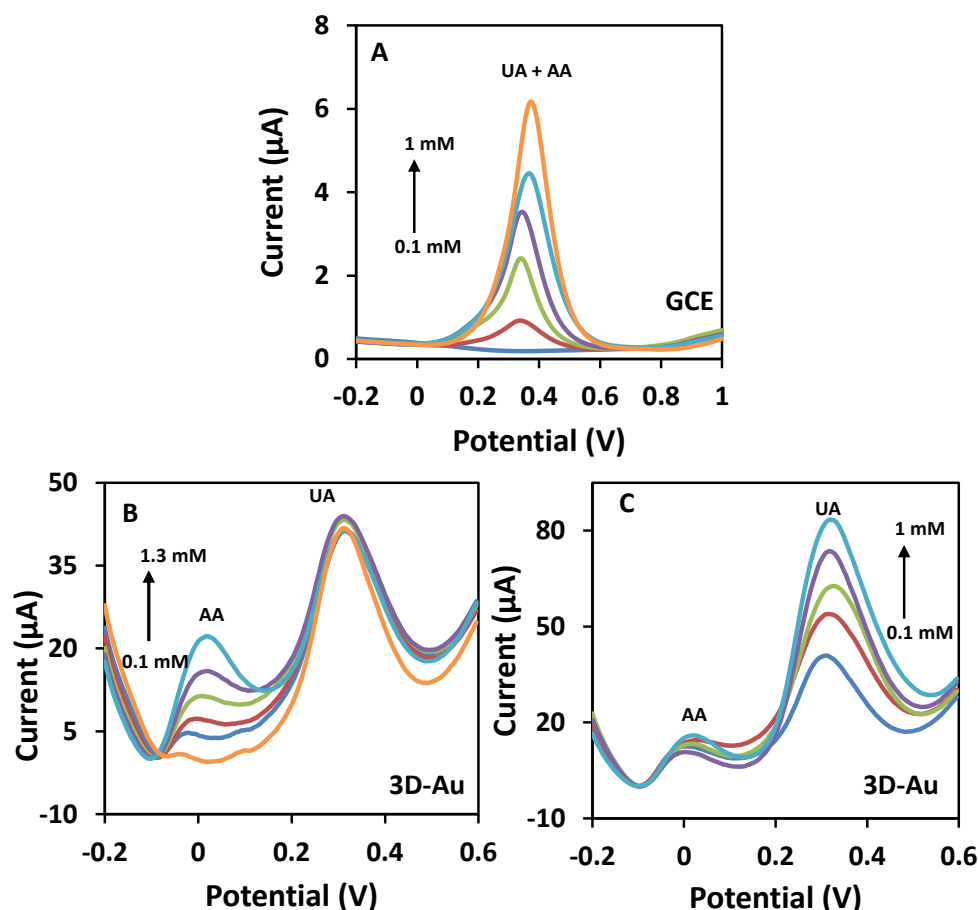


**Figure 6.** A) DPV profile of different concentration of UA (0.1 mM, 0.3 mM, 0.5 mM, 0.7 mM and 1 mM) with increasing concentration of UA (0.1 mM, 0.3 mM, 0.5 mM, 0.7 mM, 1 mM) in 0.1 M PBS (pH 7.2) on GCE. B) DPV profile of 0.1 mM UA with different concentrations of AA (0.3 mM, 0.5 mM, 0.7 mM, 1 mM and 1.3 mM) in 0.1 M PBS (pH 7.2) on 3D-printed Au electrode. C) DPV profile of 0.1 mM AA with different concentration of UA (0.1 mM, 0.3 mM, 0.5 mM, 0.7 mM, 1 mM) in 0.1 M PBS (pH 7.2) on 3D-printed Au electrode.

Calibration curves obtained for the individual and the simultaneous biomarkers detection were compared (Figure 7). It could be observed that the slope of AA in the presence of 0.1 mM UA was approximately 22% lower as compared to the slope of pure AA which is also reflected in a higher LOD. Such variations are most likely due to the presence of UA in the solution that might prohibit the free diffusion of AA to the electrode surfaces in some extent. Moreover, the anodic peak current of AA was found to be highly influenced by small changes in pH therefore, in the presence of 0.1 mM UA, the pH of the analyte would be considerably lower giving rise to such a difference in the calibration plot [26]. Such discrepancy was not observed in the calibration plots of UA since it resulted almost overlapping with that of pure UA with only 4% difference in the slope and 4% dissimilarity in detection limits (Figure 7B). The electrochemical detection and quantification of these biomarkers is possible and reliable through standard addition method using the 3D-printed Au electrode.

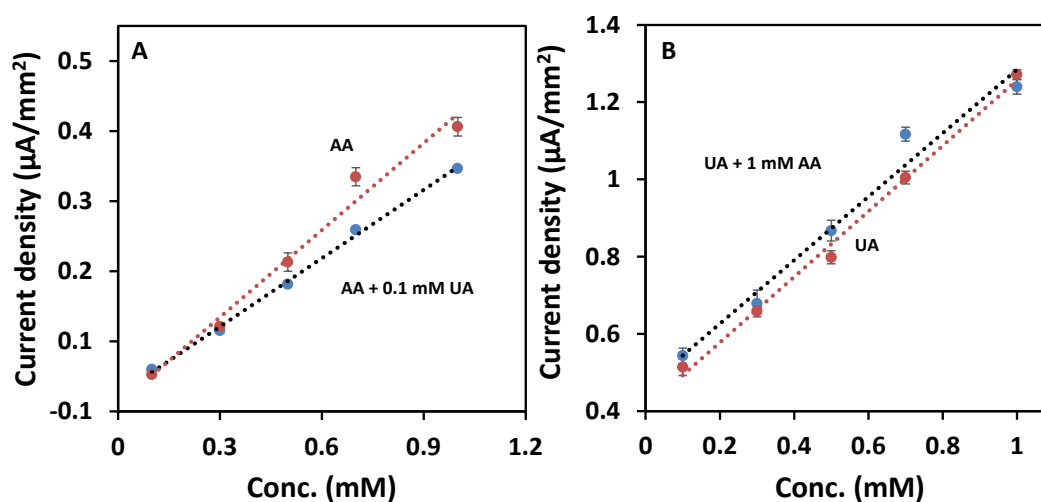


**Figure 7.** A) Plots of the oxidation current density as a function of AA concentration (0.1 mM to 1mM) with and without the presence of UA concentration (0.1 mM) with error bars included on 3D-printed Au electrode. B) Plots of the oxidation current density as a function

of UA concentration (0.1 mM to 1mM) with and without presence of AA concentration (1 mM) with error bars included on 3D-printed Au electrode.

### ***Real Sample analysis by standard addition method***

The possibility of using 3D-printed Au electrode for the determination of AA in real sample such as vitamin C tablet, VITACIMIN was tested using DPV and standard addition method [39-41]. AA concentration in the tablet was found to be 285 mM which differed from the manufacturer claim of 283 mM by only about 0.5%. Therefore, the 3D-printed Au electrode exhibits relatively good electrocatalytic activity with high accuracy in real sample analysis.

## **CONCLUSION**

In comparison with the conventionally used GCE, the gold-plated 3D-printed steel electrode exhibited excellent electrocatalytic properties in both individual and simultaneous detection of AA and UA at concentration within the biological range. Several analytical parameters such as sensitivity, selectivity, and linearity extracted from the calibration plot demonstrated the superior performance of the 3D-printed Au electrode as compared to GCE. These studies demonstrated that the 3D-printed electrode have vast potential in the field of electrochemistry for the fabrication of efficient and reusable electrochemical transducers for sensing and biosensing devices.

## EXPERIMENTAL SECTION

**Materials.** Taken in consideration of the pH value of human urine and blood which approximately ranges from 6.5 – 7.4, phosphate buffer solution (PBS) was prepared from  $\text{Na}_2\text{HPO}_4$  solution and the pH was adjusted to 7.2 with  $\text{KH}_2\text{PO}_4$  solution. 0.1mM PBS buffer of pH 7.2 was prepared and selected as the electrolyte solution for present experiments. Ascorbic Acid (AA), Uric Acid (UA), Potassium ferricyanide,  $\text{K}_3[\text{Fe}(\text{CN})_6]$ , Potassium hydroxide, KOH, and Hydrogen peroxide,  $\text{H}_2\text{O}_2$  (0.1 M) were of analytical reagent grade purchased from Sigma Aldrich and were directly used without any further purification. The stock solution of Ascorbic Acid (AA, 50 mM) and Uric Acid (UA, 15 mM) were prepared freshly using PBS buffer (0.1M, pH 7.2). 500 mg Vitamin C tablet, *VITACIMIN*, manufactured by Takeda Indonesia was selected as a real sample. The sample underwent physical purification steps before the content of AA was electrochemically determined.

**Apparatus.** Conventional three-electrode configuration was used in every electrochemical measurement. Pt wire was used as an auxiliary electrode; Ag/AgCl served as a reference electrode; glassy carbon (GCE) electrode (3 mM in Diameter) or 3D-printed Au electrode was selected as working electrodes (Figure S2 of Supporting information). The cyclic voltammetry (CV) and differential pulse voltammetry (DPV) were conducted using a  $\mu$ Autolab Type III electrochemical analyser (Eco Chemie, The Netherlands) supported by NOVA 1.10 software (Eco Chemie). A JEOL 7600F Schottky field emission scanning electron microscope (JEOL Ltd., Tokyo, Japan) was used for the SEM-EDX.

## Procedure

**Modification of the 3D-printed Stainless Steel electrode surface with Au by electroplating.** Au electroplated electrodes were obtained as previously reported [30]. Briefly, the stainless steel electrode was immersed into a commercial gold plating and the deposition

was carried out by applying a current of -20 mA for 90 min while stirring in the presence of a Ag/AgCl reference electrode and a platinum auxiliary electrode.

**Cleaning method of 3D-Printed Au Electrode.** Prior to measurement, the 3D-printed Au electrode was immersed into a solution of KOH (50 mM) and H<sub>2</sub>O<sub>2</sub> (25% v/v) for 10 min. After this treatment, the electrode was placed in KOH solution (50 mM) and a potential sweep from -200 to -1200 mV (vs Ag/AgCl) was conducted at a scan rate of 50 mV/s [42]. The 3D-printed Au electrode was then rinsed with deionised water and dried using nitrogen gas.

**Real sample preparation.** Taken into consideration that AA exhibits high solubility properties in water (~1.7 M)<sup>1</sup>, 500 mg Vitamin C Tablet, *VITACIMIN*, was directly added into PBS buffer (0.1M), followed by centrifuging at 8000 rpm for 10 min. After which, the supernatant was filtered and further diluted..

**Electrochemical measurement.** Three-electrode configuration was used and immersed into an electrochemical cell containing analyte of interest (7 mL). After recording blank voltammogram 0.1 M PBS (pH 7.2), aliquots of target biomarker analyte (AA, UA) were subsequently introduced to acquire the following concentration, 0.1 mM, 0.3 mM, 0.5 mM and 1mM. A scan rate of 0.1 V/s was used in CV measurement. DPV measurement parameters were as follows: 0.025 V modulation amplitude, 0.05 s modulation time, 0.005 V for step potential adopting scan rate of 0.01 V/s. All electrochemical measurements were reported vs. the Ag/AgCl reference electrode and were conducted in room temperature (25 ± 2 °C). Prior to measurement, GCE surface (3mm in Diameter) was polished sequentially with alumina powder (0.05 µm) on a polishing pad which was rinsed thoroughly with deionised water and dried to obtain a clean mirror finish. The 3D-printed Au electrode underwent the cleaning procedure as mentioned. Each electrochemical measurement was repeated three

times to obtain the standard deviation to ensure the reproducibility of the results. In between each voltammetry scan, GCE surface was polished and rinsed with deionised water. While the 3D-printed Au electrode was rinsed with deionised water and dried using nitrogen gas.

The active surface area of the 3D-printed Au electrode that participated in the redox reaction was dictated by the peak current intensity at various scan rate of  $\text{K}_3[\text{Fe}(\text{CN})_6]$  (1 mM) in KCl (0.1 M) and with the use of Randles-Sevcik equation. The diffusion coefficient value is  $7.2 \times 10^{-6} \text{ cm}^2 \text{ s}^{-1}$  and was obtained from the literature[43].

## Acknowledgments

M.P. thanks Tier 1 (123/16) grant from ministry of Education, Singapore.

## REFERENCES

- [1] A. Apelblat, E. Manzurola, Solubility of ascorbic, 2-furancarboxylic, glutaric, pimelic, salicylic, and o-phthalic acids in water from 279.15 to 342.15 K, and apparent molar volumes of ascorbic, glutaric, and pimelic acids in water at 298.15 K, *The Journal of Chemical Thermodynamics* 21 (1989) 1005-1008.
- [2] S. Nakamura, T. Oku, Bioavailability of 2-O-alpha-D-glucopyranosyl-L-ascorbic acid as ascorbic acid in healthy humans, *Nutrition* 25 (2009) 686-691.
- [3] A. Meister, Glutathione Ascorbic-Acid Antioxidant System In Animals, *Journal of Biological Chemistry* 269 (1994) 9397-9400.
- [4] R.E. Hodges, J. Hood, J.E. Canham, H.E. Sauberlich, E.M. Baker, Clinical manifestations of ascorbic acid deficiency in man, *The American journal of clinical nutrition* 24 (1971) 432-443.
- [5] J. Maiuolo, F. Oppedisano, S. Gratteri, C. Muscoli, V. Mollace, Regulation of uric acid metabolism and excretion, *International Journal of Cardiology* 213 (2016) 8-14.
- [6] A.C.M. Gagliardi, M.H. Miname, R.D. Santos, Uric acid: A marker of increased cardiovascular risk, *Atherosclerosis* 202 (2009) 11-17.
- [7] S. Škrovánková, J. Mlček, J. Sochor, M. Baroň, J. Kynický, T. Juríková, Determination of ascorbic acid by electrochemical techniques and other methods, *International Journal of Electrochemical Science* (2015).
- [8] T. Zhang, X. Sun, B. Liu, Synthesis of positively charged CdTe quantum dots and detection for uric acid, *Spectrochim Acta A Mol Biomol Spectrosc* 79 (2011) 1566-1572.
- [9] M.R. Moghadam, S. Dadfarnia, A.M. Shabani, P. Shahbazikhah, Chemometric-assisted kinetic-spectrophotometric method for simultaneous determination of ascorbic acid, uric acid, and dopamine, *Anal Biochem* 410 (2011) 289-295.

- [10] H. Zhou, Sensitive Electrochemical Determination Uric Acid at Pt Nanoparticles Decorated Graphene Composites in the Presence of Dopamine and Ascorbic Acid, *International Journal of Electrochemical Science* (2016) 5197-5206.
- [11] S. Thiagarajan, S.M. Chen, Preparation and characterization of PtAu hybrid film modified electrodes and their use in simultaneous determination of dopamine, ascorbic acid and uric acid, *Talanta* 74 (2007) 212-222.
- [12] M.Z. Nasir, Z. Sofer, A. Ambrosi, M. Pumera, A limited anodic and cathodic potential window of MoS<sub>2</sub>: limitations in electrochemical applications, *Nanoscale* 7 (2015) 3126-3129.
- [13] J.B. Raoof, R. Ojani, M. Baghayeri, A selective sensor based on a glassy carbon electrode modified with carbon nanotubes and ruthenium oxide/hexacyanoferrate film for simultaneous determination of ascorbic acid, epinephrine and uric acid, *Analytical Methods* 3 (2011) 2367-2373.
- [14] L.M. Niu, K.Q. Lian, H.M. Shi, Y.B. Wu, W.J. Kang, S.Y. Bi, Characterization of an ultrasensitive biosensor based on a nano-Au/DNA/nano-Au/poly(SFR) composite and its application in the simultaneous determination of dopamine, uric acid, guanine, and adenine, *Sensors and Actuators B-Chemical* 178 (2013) 10-18.
- [15] W.H. Cai, T. Lai, H.J. Du, J.S. Ye, Electrochemical determination of ascorbic acid, dopamine and uric acid based on an exfoliated graphite paper electrode: A high performance flexible sensor, *Sensors and Actuators B-Chemical* 193 (2014) 492-500.
- [16] M.A. Gilmartin, J.P. Hart, B. Birch, Voltammetric and amperometric behaviour of uric acid at bare and surface-modified screen-printed electrodes: studies towards a disposable uric acid sensor, *Analyst* 117 (1992) 1299-1303.
- [17] J.-M. Zen, C.-T. Hsu, A selective voltammetric method for uric acid detection at Nafion®-coated carbon paste electrodes, *Talanta* 46 (1998) 1363-1369.
- [18] Z.H. Sheng, X.Q. Zheng, J.Y. Xu, W.J. Bao, F.B. Wang, X.H. Xia, Electrochemical sensor based on nitrogen doped graphene: simultaneous determination of ascorbic acid, dopamine and uric acid, *Biosens Bioelectron* 34 (2012) 125-131.
- [19] C. Wang, J. Du, H. Wang, C.e. Zou, F. Jiang, P. Yang, Y. Du, A facile electrochemical sensor based on reduced graphene oxide and Au nanoplates modified glassy carbon electrode for simultaneous detection of ascorbic acid, dopamine and uric acid, *Sensors and Actuators B: Chemical* 204 (2014) 302-309.
- [20] J. Li, Y. Wang, Y. Sun, C. Ding, Y. Lin, W. Sun, C. Luo, A novel ionic liquid functionalized graphene oxide supported gold nanoparticle composite film for sensitive electrochemical detection of dopamine, *RSC Adv.* 7 (2017) 2315-2322.
- [21] C. Wang, R. Yuan, Y. Chai, S. Chen, F. Hu, M. Zhang, Simultaneous determination of ascorbic acid, dopamine, uric acid and tryptophan on gold nanoparticles/overoxidized-polyimidazole composite modified glassy carbon electrode, *Analytica chimica acta* 741 (2012) 15-20.
- [22] A. Ambrosi, M.T. Castaneda, A.J. Killard, M.R. Smyth, S. Alegret, A. Merkoci, Double-codified gold nanolabels for enhanced immunoanalysis, *Anal Chem* 79 (2007) 5232-5240.
- [23] M. Pumera, X. Llopis, A. Merkoçi, S. Alegret, Microchip capillary electrophoresis with a single-wall carbon nanotube/gold electrochemical detector for determination of aminophenols and neurotransmitters, *Microchimica Acta* 152 (2006) 261-265.
- [24] M. Pumera, J. Wang, E. Grushka, R. Polsky, Gold nanoparticle-enhanced microchip capillary electrophoresis, *Analytical chemistry* 73 (2001) 5625-5628.
- [25] M.-C. Daniel, D. Astruc, Gold nanoparticles: assembly, supramolecular chemistry, quantum-size-related properties, and applications toward biology, catalysis, and nanotechnology, *Chem Rev* 104 (2004) 293-346.

- [26] G. Hu, Y. Ma, Y. Guo, S. Shao, Electrocatalytic oxidation and simultaneous determination of uric acid and ascorbic acid on the gold nanoparticles-modified glassy carbon electrode, *Electrochimica Acta* 53 (2008) 6610-6615.
- [27] A. Ambrosi, C.K. Chua, N.M. Latiff, A.H. Loo, C.H.A. Wong, A.Y.S. Eng, A. Bonanni, M. Pumera, Graphene and its electrochemistry - an update, *Chem Soc Rev* 45 (2016) 2458-2493.
- [28] X. Tian, C. Cheng, H. Yuan, J. Du, D. Xiao, S. Xie, M.M. Choi, Simultaneous determination of l-ascorbic acid, dopamine and uric acid with gold nanoparticles- $\beta$ -cyclodextrin-graphene-modified electrode by square wave voltammetry, *Talanta* 93 (2012) 79-85.
- [29] A. Ambrosi, M. Pumera, 3D-printing technologies for electrochemical applications, *Chem Soc Rev* 45 (2016) 2740-2755.
- [30] A.H. Loo, C.K. Chua, M. Pumera, DNA biosensing with 3D printing technology, *Analyst* (2017).
- [31] K.Y. Lee, A. Ambrosi, M. Pumera, 3D-printed Metal Electrodes for Heavy Metals Detection by Anodic Stripping Voltammetry, *Electroanalysis* 29 (2017) 2444-2453.
- [32] T.S. Cheng, M.Z.M. Nasir, A. Ambrosi, M. Pumera, 3D-printed metal electrodes for electrochemical detection of phenols, *Appl Mater Today* 9 (2017) 212-219.
- [33] G. Tan, M.Z.M. Nasir, A. Ambrosi, M. Pumera, 3D Printed Electrodes for Detection of Nitroaromatic Explosives and Nerve Agents, *Anal Chem* 89 (2017) 8995-9001.
- [34] B.R. Liyarita, A. Ambrosi, M. Pumera, 3D-printed Electrodes for Sensing of Biologically Active Molecules, *Electroanalysis* DOI: 10.1002/elan.201700828.
- [35] A. Ambrosi, J.G.S. Moo, M. Pumera, Helical 3D-Printed Metal Electrodes as Custom-Shaped 3D Platform for Electrochemical Devices, *Adv Funct Mater* 26 (2016) 698-703.
- [36] A. Ambrosi, M. Pumera, Self-Contained Polymer/Metal 3D Printed Electrochemical Platform for Tailored Water Splitting, *Adv Funct Mater* DOI: 10.1002/adfm.201700655.
- [37] R.G. Compton, F.M. Matysik, Sonovoltammetric behavior of ascorbic acid and dehydroascorbic acid at glassy carbon electrodes: analysis using pulsed sonovoltammetry, *Electroanalysis* 8 (1996) 218-222.
- [38] G. Dryhurst, N.T. Nguyen, M.Z. Wrona, R.N. Goyal, A. Brajtertoth, J.L. Owens, H.A. Marsh, Elucidation of the biological redox chemistry of purines using electrochemical techniques, *Journal of Chemical Education* 60 (1983) 315-319.
- [39] A. Safavi, N. Maleki, O. Moradlou, F. Tajabadi, Simultaneous determination of dopamine, ascorbic acid, and uric acid using carbon ionic liquid electrode, *Anal Biochem* 359 (2006) 224-229.
- [40] M. Bader, A systematic approach to standard addition methods in instrumental analysis, *J. Chem. Educ* 57 (1980) 703.
- [41] B.E. Saxberg, B.R. Kowalski, The Generalized Standard Addition Method, in, *WASHINGTON UNIV SEATTLE LAB FOR CHEMOMETRICS*, 1978.
- [42] L.M. Fischer, M. Tenje, A.R. Heiskanen, N. Masuda, J. Castillo, A. Bentien, J. Émneus, M.H. Jakobsen, A. Boisen, Gold cleaning methods for electrochemical detection applications, *Microelectronic Engineering* 86 (2009) 1282-1285.
- [43] S. Konopka, B. McDuffie, Diffusion coefficients of ferri- and ferrocyanide ions in aqueous media, using twin-electrode thin-layer electrochemistry, *Analytical Chemistry* 42 (1970) 1741-1746.

## Graphical abstract

